A Lossless Hybrid Shape-Adaptive Image Coder

J. Wang, P. Ogunbona and G. Naghdy

Department of Electrical & Computer Engineering University of Wollongong Australia

Lossless image compression continues to be the focus of the medical picture archiving system designers because of the possibility of reducing the bandwidth required to transmit medical images. The lossless Differential Pulse Code Modulation (DPCM) and Hierarchical Interpolation (HINT) have been suggested as solutions to this problem. However, there are limitations due to the inability of these schemes to adapt to local image statistics. Efforts to alleviate this problem can be seen in various adaptive schemes found in the literature. This paper introduces a new adaptive DPCM (ADPCM) scheme based on the shape of the region of support (ROS) of the predictor. The shape information of the local region is obtained through a universal Vector Quantization (VQ) scheme. The proposed lossless encoding scheme switches predictor type depending on the local shape. Simulation results show that improvements of about 0.4 bits/pixel over basic DPCM and 0.2 bits/pixel over HINT can be obtained. Comparison with lossless JPEG indicates that the proposed scheme can cope more easily with the changes in local image statistics. The computation required is moderate, since a universal VQ is used in encoding the shape information.

Keywords: Medical images, Lossless coding, Adaptive DPCM, Shape VQ.

1. Introduction

Digital imaging techniques are increasingly more common in medical applications and there is a consequent need to find economical ways of storing the acquired visual data. Coupled with this need for storage is the requirement to preserve the integrity of medical images after reconstruction. Suitable storage mechanism is provided through lossless compression of the images. However, the compression ratio that can be obtained through lossless compression is not comparable to those reported for lossy schemes. Most of the lossless schemes are based on some form of prediction, while the lossy schemes take advantage of such methods as transform and wavelet coding, and vector quantisation. The lossless variant of DPCM is the most common form of the lossless image compression: the lossless JPEG compression algorithm is a variant of DPCM.

Several variants of DPCM have been reported in the literature [Habibi 1971, Jain 1989, Hsieh et al. 1989, Prabhu 1985, Maragos 1984, Zschunke 1977]. For image data, the effectiveness of DPCM as a coding algorithm stems from the inherent inter-pixel redundancy. Success of the lossless variant of DPCM depends on the degree to which the predictor is able to model the image data, thereby yielding a low variance of estimation error. In a lossless coder this error needs to be encoded as well for use in the accurate reconstruction of the data.

The fact that images are non-stationary makes straightforward prediction ineffective, especially at edge locations. Model-based approaches have been used to overcome this problem [Das and Burgett 1993]. Recently, context-based and segmentation-based methods have been proposed to adaptively predict the pixels in the edge area [Shen and Rangayyan 1997, WU 1997]. In this paper, a novel adaptive hybrid DPCM scheme modifying the order of prediction based on the shape of the edge is developed.

The rest of the paper is organized as follows. In Section 2, DPCM coding is briefly reviewed. In sections 3, 4 and 5, the proposed scheme is introduced. A performance comparison between the new DPCM coder and other lossless predictive coders is given in section 6. The results are

presented in Section 7, while a discussion and further development are given in Section 8.

2. A Review of DPCM Image Coding

Two-dimensional linear prediction often employs the auto-regressive (AR) model in generating the estimate of an image pixel $f(i,j)$:

$$\tilde{f}(i,j) = \sum\sum a(p,q) f(i-p,j-q),\ (p,q) \in \tilde{S} \quad (1)$$

where $(p,q) \neq (0,0)$, and $\tilde{f}(i,j)$ is the predicted value of the pixel. In (1), $a(p,q)$ are the prediction coefficients and $\tilde{S}$ is the region of support (ROS). If the ROS is *strongly causal* as depicted by Jain [Jain 1989 pp. 205], the prediction model is often called the non-symmetric half-plane (NSHP) model.

The prediction error, $\varepsilon(i,j)$ is given as:

$$\varepsilon(i,j) = f(i,j) - \tilde{f}(i,j) \quad (2)$$

In a DPCM algorithm the prediction errors are stored instead of the image data, and, because the variance of $\varepsilon(i,j)$ is much smaller than that of the raw image pixels, compression is achieved.

The basic DPCM method utilises fixed prediction coefficients irrespective by of the local statistics of the pixel or the region being encoded. Its advantages are ease of implementation and little computational overhead. However, because of the non-stationary nature of image data, a fixed set of prediction coefficients cannot sufficiently model the data, especially at the edges. Several methods have been developed to include the concept of adaptivity in DPCM schemes [Hibibi 1977, Hsieh et al. 1989, Kuduvalli and Rangayyan 1992, Prabhu 1985, Maragos et al. 1984, Roos et al. 1988, Zschunke 1977]. There are two classes of methods [Hibibi 1977]: DPCM with adaptive prediction coefficients [Kuduvalli and Rangayyan 1992, Prabhu 1985, Maragos et al. 1984, Roos et al. 1988, Zschunke 1977], and DPCM with an adaptive quantizer [Hibibi 1977].

When adapting the prediction coefficients optimal values can be obtained for each pixel [Prbhu 1985, Roos et al. 1988, Zschunke 1977], or on a block basis [Hsieh et al. 1989, Maragos et al. 1984, Kuduvalli and Rangayyan 1992]. Coefficients are obtained on a block basis in the two-dimensional multiplicative autoregressive model-based (MAR) coder proposed by Das and Burgett [Das and Burgett 1993] as well, but it utilises the MAR model and is not considered as the variant of DPCM. In the method of Roos et al. [Roos et al. 1988] the computation of the coefficients to be used in the prediction of the current pixel is based on the neighbouring pixels. Adaptivity was achieved in the methods of Zschunke [Zschunke 1977] and Prabhu [Prabhu 1985] by basing the choice of predictors on the relationship between the current pixel and the pixels in its neighbourhood. The choice of the predictor for the current pixel needs to be transmitted as overhead. By assuming that local stationarity holds over a block of pixels, optimal prediction coefficients can be computed for each block and used in the prediction of the pixels within the block. The coefficients of each block also need to be transmitted. A large overhead is incurred in terms of the side information that needs to be transmitted. Further, the non-stationarity of the data in blocks containing edges results in high prediction error values and detracts from the value of these adaptive schemes for lossless DPCM.

Adaptivity of the quantizer is attractive for a lossy DPCM scheme [Habibi 1977], but inappropriate in the lossless scheme, because the error signal must be reconstructed without loss.

3. Shape-adaptive DPCM

A new linear prediction scheme, the shape-adaptive DPCM (SADPCM), is presented in this paper. Its suitability in a lossless DPCM compression algorithm stems from the high-performance prediction and low computational requirement.

The basic DPCM procedure is able to decorrelate pixels in a smooth image region and performs poorly in areas with low correlation, because the pixels are unpredictable. DPCM with constant prediction order will produce non-stationary errors. In the proposed method, the coder adjusts the predictor adaptively pixel-wise as the correlation of the pixels alters. Figure 1 depicts eight possible relationships that

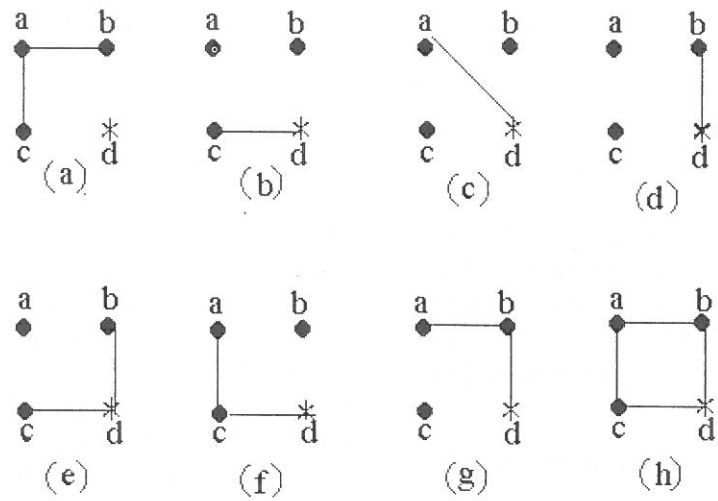

Fig. 1. Eight possible relationships between a given pixel and the pixels in its ROS.

can exist between a given pixel and its neighbours in a 2*2 ROS.

In Figure 1, "* " denotes the current pixel, $f(i,j)$, to be predicted. The pixels used in the prediction are denoted as "•"; they are the pixels $f(i-1,j)$, $f(i,j-1)$ and $f(i-1,j-1)$ and they constitute the ROS. Here, the ROS is strict NSHP and is a third-order predictor [Habibi 1971]. The lines joining pixels imply that there is a high correlation among the joined pixels, otherwise no useful relationship exists between the pixel to be predicted and the predictor pixels. Correlation between two pixels is assumed to depend on their grey scale values and a high correlation is defined as two pixels having identical or close values.

The ROS is chosen as NSHP 2*2 for two reasons. First, NSHP ensures that all the pixels in the ROS have appeared before the current pixel in a raster scan of the image. The order of scanning is from left to right and from top to bottom. This will ensure that every pixel except those in the first column and the first row can be predicted and reconstructed without any problems. The second reason is that a third-order predictor is adequate for decorrelating inter-pixel redundancy [Habibi 1971, Jain 1989 pp. 491, Zschunke 1977]. Using few parameters also simplifies the system from an implementation viewpoint.

The structures depicted in Figure 1 are now considered in terms of prediction. In fact, the required predictors will change as the correlation between the pixels varies. In Figure 1 (a), the pixel being predicted has no correlation with the pixels in the ROS. For this kind of pixels, a special strategy of prediction based on VQ will be exploited; this is presented in Section 5. In Figures 1 (b) – (d), the pixel being predicted has a correlation with only one of the pixels in the ROS. A first-order predictor is applied in this case:

$$\tilde{f}(i,j) = f(i-p,j-q), \tag{3}$$

where $p,q \in [0,1]$ and $(p,q) \neq (0,0)$. In Figures 1 (e) – (g), the pixel to be predicted is correlated with two out of the three pixels in the support region. Under such condition, a second-order predictor is appropriate:

$$\tilde{f}(i,j) = \frac{f(i-p,j-q)+f(i-r,j-s)}{2}, \tag{4}$$

where $p,q,r,s \in [0,1]$, $(p,q) \neq (0,0)$, $(r,s) \neq (0,0)$, and $(p,q) \neq (r,s)$. Finally, for those pixels with a correlation structure as depicted in Figure 1 (h), a third-order predictor is used [Roos et al. 1988]:

$$\tilde{f}(i,j)=[0.95*f(i,j-1)+0.95*f(i-1,j) -0.95*0.95*f(i-1,j-1)]/[0.95*(2-0.95)]. \tag{5}$$

In this way, the order of prediction switches based on the shape of the set of correlated pixels within the 2*2 ROS; linear prediction is applied adaptively. A higher accuracy of prediction is obtained because only highly correlated pixels are used.

Codebook size	A128	A256	A512	U128	U256	U512	U1024
SNR	29.5	31.2	31.5	28.2	30.6	31.3	31.9

Table 1. SNR of the shape vectors of "Lena " using different codebook sizes.

Unresolved issues about the proposed scheme include (i) how to transmit the choice of predictors without much overhead, and (ii) how to obtain information about the local shape. These will be resolved in the next sections of the paper.

4. Vector Quantization of the Shape Information

VQ is an effective tool in lossy image compression. It can be described as mapping of a K-dimensional Euclidean space R^k into a finite subset C, the codebook, containing N reproduction points called code vectors [Grey 1984]. In VQ image coding, the image is divided into small blocks of which the input vectors are formed; each input vector is encoded by the index of the code vector to which it is closest according to a distortion function. Vector quantization can further be described as a pattern classification technique and has also been used in hybrid image coding schemes with other methods, such as Discrete Cosine Transform (DCT) coding [Cowman et al. 1984]. In this paper, VQ is used as a tool to acquire the local shape of image blocks.

In the proposed scheme, the original image is first divided into non-overlapping blocks of 8*8 pixels. The mean of each block is computed and removed from the pixel values (mean normalisation). This process removes the bias of the block mean and reveals the shape or structure of the block.

The shape vectors can be grouped together using a universal or image-adaptive codebook. For each input shape vector, the index of the nearest code vector in the codebook stores its information. VQ is used in this situation as a quantizer of the shape information of the image blocks. The problem posed in the previous section on how to easily obtain the information about the local shape without much overhead is thus resolved by VQ.

A universal codebook is employed in this work because of the low overhead when compared to an image-adaptive codebook. This is even more so because of the premium placed on the use of available bits budget. The adaptive codebook leads to less distortion as it more closely models the input vectors; a large universal codebook can be used to solve this problem. Table 1 shows how the fidelity of representation of the shapes, measured in terms of signal-to-noise-ratio (SNR), increases as the codebook size increases. The SNR here is calculated as:

$$\mathrm{SNR}(dB)=10*\log\left\{\frac{\sum_{i=0}^{255}\sum_{i=0}^{255} f_i^2(i,j)}{\sum_{i=0}^{255}\sum_{i=0}^{255}[f_i(i,j)-f_c(i,j)]^2}\right\} \quad (6)$$

where $f_i(i,j)$ is the value in the shape vector at location (i,j), $f_c(i,j)$ is the corresponding value in the code vector. The test image "*Lena*" with a size 256*256 pixels has been used.

In Table 1, the prefix "A " indicates that an adaptive codebook is used while the prefix "U " indicates a universal codebook; the number is the size of the codebook.

From the results of Table 1, which show the same trend as with other test images, it can be seen that both codebook types can produce almost the same SNR for sizes greater than 256. In this paper, a codebook of 256 shape code vectors (8*8 pixels) generated using the LBG algorithm [GREY 1984] is used. The training sequence consists of vectors derived from 15 images.

5. Lossless Hybrid Shape-Adaptive DPCM (SADPCM)/DPCM/VQ Encoder

At the encoder of the proposed system, the image is initially decorrelated using DPCM with a predictor, as shown in (5), and the prediction errors are stored. The original image is then split into 8*8 non-overlapping blocks, and the shape vectors are formed by mean normalisation. VQ

is applied to each shape vector and the resulting indices are stored as side information.

Each 8*8 image block is further divided into four 4*4 blocks and SADPCM is applied to these blocks. Furthermore, the 4*4 blocks are classified as either a high or low activity block, depending on the absolute value of the DPCM prediction errors in each block. If there are errors whose absolute values exceed the threshold, the block is labelled as high activity type and denoted "1", otherwise it is labelled as a low activity type and denoted "0". The one bit index ("0 " or "1") is also stored as side information. For the low activity blocks, the errors of DPCM are stored and SADPCM is applied to the rest of the blocks. In this scheme, DPCM is used both as a predictor and as the indicator. For the smooth regions in an image DPCM is still one of the best coders for lossless coding; in such regions DPCM outperforms SADPCM/VQ, because the shape of the block is not exactly represented by the code vector.

The choice of the threshold by which the block is classified as "1 " or "0 " depends on the level of noise in the image; the level of noise is reflected by the prediction errors. In this research, the noise level of the "simple " images is within the range $[-1, 1]$. So, in this kind of images, only those prediction errors with absolute values greater than one are initiated by the DPCM itself. The threshold for these images is chosen as unity. For "complex " images, the noise level tends to be in the interval [-5, 5]. So, five is the choice of the threshold for these images. The "simple " and "complex " images are defined by the histogram of the DPCM-based prediction errors. There are two types of histograms of absolute errors of images, as shown in Figure 2.

Images with prediction error histograms as in Figure 2 (a) are categorised as "simple". In these images, the number of error samples whose absolute values are unity is smaller than the number of errors with a value of zero and the threshold is set as unity. The other type of images categorised as "complex " have an error histogram as shown in Figure 2 (b) and the threshold is set as five. Errors above the threshold are caused by the inability of DPCM to properly model the image region under consideration. In these situations the blocks are decorrelated by SADPCM.

The size of the shape vector is chosen as 8*8 instead of 4*4 because of the bits saved in representing the side information. For example, a codebook of 256, 4*4 code vectors requires 8 bits per vector or 0.5 bits per pixel, whereas using an 8*8 code vector requires 8 bits per vector or 0.125 bits per pixel.

In applying SADPCM to each pixel in high activity regions, the shape pixels in the code vector are used. The current pixel and its 2*2 ROS in the code vector are evaluated for correlation; a simple difference calculation is used. For example, using the 2*2 block of Figure 3, the absolute difference between pixel $f(i,j)$ and each of the pixels in the ROS in the code vector is calculated as:

$$\vec{e}(i,j) = |\vec{f}(i,j) - \vec{f}(i-p, j-q)|, \qquad (7)$$

where $\vec{e}(i,j)$ is the difference and $p, q \in [0, 1]$, $(p,q) \neq (0,0)$.

Here, in Figure 3 (b), the three differences are 0, 0.5 and 0. Correlation in this context is defined as the difference being less than some threshold;

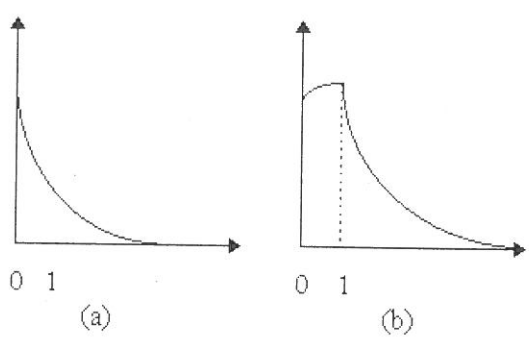

Fig. 2. Two kinds of histograms of the absolute errors of DPCM.

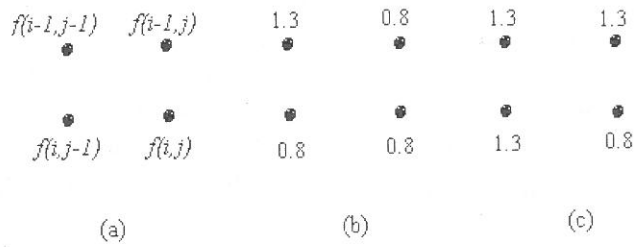

Fig. 3. Two 2*2 blocks in the original image and their corresponding pixels in the codebook.

otherwise there is no correlation. The threshold here is set as 0.2 by experimentation. As the threshold increases, pixels with little correlation may be included for the prediction; decreasing of the threshold will exclude those pixels with high correlation. In both cases, performance of the predictor will be degraded. In the example given, pixel $f(i-1,j-1)$ has no correlation with pixel $f(i,j)$; this situation is equivalent to the decision rule given in Section 3 in which the predictor of (4) is used.

If it is found in the code vector in Figure 3 (c) that $f(i,j)$ has no correlation with any of the pixels in the ROS, which is the case in Figure 1 (a), the predictor uses VQ in the following manner. Recall that each element of the shape vector is mean normalised. Then, the four pixels in Figure 3 are related according to:

$$\frac{f(i-1,j-1)}{f'(i-1,j-1)} = \frac{f(i-1,j)}{f'(i-1,j)} = \frac{f(i,j-1)}{f'(i,j-1)} = \frac{f(i,j)}{f'(i,j)} = \mu_b, \quad (8)$$

where μ_b is the block mean, $f(i-1,j)$, $f(i,j-1)$, $f(i-1,j-1)$ and $f(i,j)$ are the raw grey scale values of the pixels which are those in Figure 3 (a), and $f'(i-1,j)$, $f'(i,j-1)$, $f'(i-1,j-1)$ and $f'(i,j)$ are the values of the shape vector pixels which are those in Figure 3 (c). Using the relationship in (8) it is possible to write:

$$\frac{\frac{f(i-1,j-1)+f(i-1,j)+f(i,j-1)}{3}}{\frac{f'(i-1,j-1)+f'(i-1,j)+f'(i,j-1)}{3}} = \frac{f(i,j)}{f'(i,j)} \quad (9)$$

The ratio on the left hand side of (9) can be interpreted as the ratio of mean of the pixel in the ROS of the predictor in both the image domain and the codebook. The predicted pixel value, $\tilde{f}(i,j)$, can now be computed from:

$$\tilde{f}(i,j) = f'(i,j) * \frac{\overline{R}}{\overline{C}} \quad (10)$$

where $\overline{R}$ is the mean of the pixels in the ROS of the predictor in image data, $\overline{C}$ is the mean of the same pixels in the mean normalised codebook, and $f'(i,j)$ is the corresponding value of the pixel being predicted in the codebook.

The flowchart of the algorithm is depicted in Figure 4. The decision rule for selecting the prediction order is listed in Table 2. At the transmitter, not only the errors of prediction but also all the side information need to be sent. The prediction errors include the errors of DPCM and those of SADPCM. The side information includes the indices of 8*8 image blocks and the labels of the 4*4 blocks. At the decoder, all the pixels can be losslessly recovered by using the errors and the side information. The whole error image is divided into 8*8 blocks, and the code vector for each block is found by the index in the side information. Each block is then split into 4*4 blocks. The index of each 4*4 block can also be found in the side information. The image, therefore, can be totally recovered by the same decision rule as introduced before.

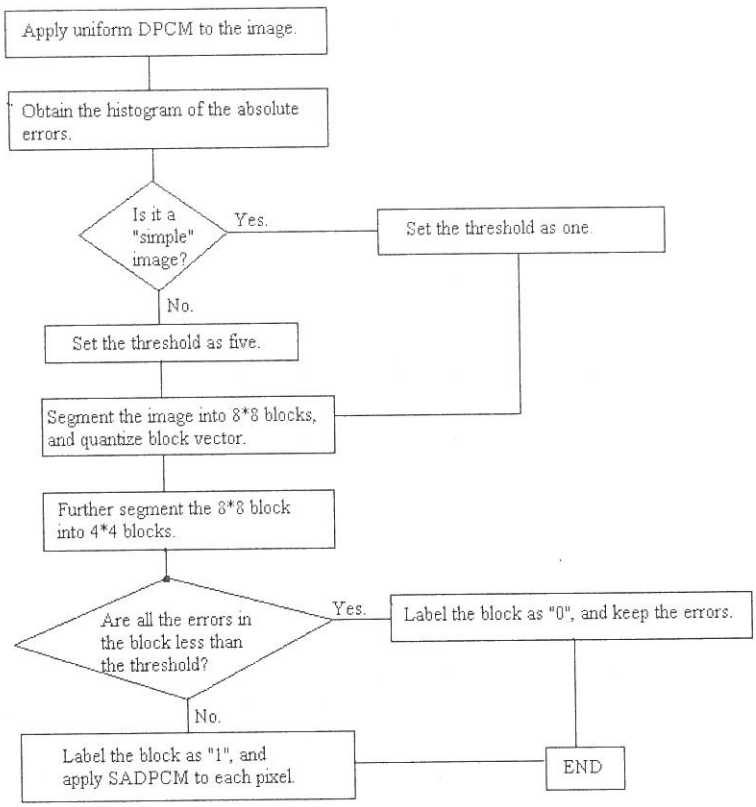

Fig. 4. Flowchart of hybrid SADPCM.

Number of pixels in the ROS that have correlation with current pixel	The optimal predictor
None (See Figure 1 (a))	VQ-based predictor (See (10))
One (See Figure 1 (b) – (d))	First-order predictor (See (5))
Two (See Figure 1 (e) – (g))	Second-order predictor (See (6))
Three (See Figure 1 (h))	Third-order predictor (See (7))

Table 2. Decision rule for selecting the "optimal " predictor.

6. Comparative Analysis of the Hybrid SADPCM Coder

In this section, the performance of hybrid SADPCM, DPCM, ADPCM (pixel-by-pixel [Prbhu 1985, ROOS et al. 1988, Zschunke 1977] and block-by-block [Hsieh et al. 1989, Maragos et al. 1984, Kuduvalli and Rangayyan 1992]) and MAR coder [Das and Burgett 1993] are compared. The DPCM coder is, no doubt, the simplest among all the predictive schemes discussed in this comparison. The problem with DPCM is, that it is unable to cope with edges using the same predictors that perform well in smooth areas; high prediction errors are thus incurred around the edges. Table 4 shows the result of testing DPCM with nine images. It is clear that most of the large errors are due to the predictor. Figure 5 shows the pixels incurring the highest prediction error in each of the nine test-images when DPCM is applied.

In Figure 5, the pixel labelled "* " is the one being predicted and those labelled "•"s form its ROS. A comparison of the prediction errors obtained using DPCM and SADPCM is given in Table 3. In Table 3, (a)-(i) are the nine pixels listed in Figure 5. The results clearly indicate that in those areas where DPCM has high prediction errors, SADPCM has significantly reduced errors.

ADPCM outperforms DPCM because the predictor adapts to the changes in local image

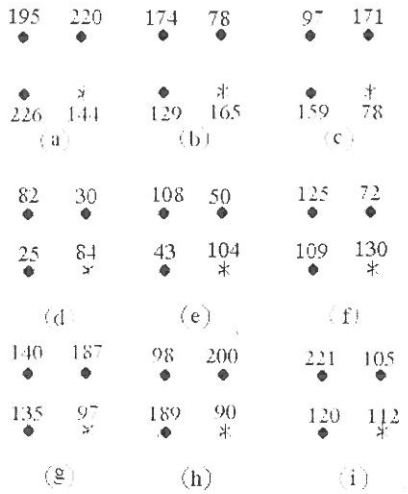

Fig. 5. The pixel with the highest error in each of the nine images and its ROS.

statistics. Traditional pixel-by-pixel ADPCM can achieve very high prediction performance [Prabhu 1985, Zschunke 1977] at the expense of huge side information, especially in a lossless coder. This problem is alleviated by using block-based adaptation in which the side information is reduced. In the schemes proposed by Kuduvalli and Rangayyan (ADPCM) [Kuduvalli and Rangayyan 1992], prediction parameters are obtained by the extended multichannel version of the Burg algorithm. Das and Burgett presented a MAR model-based predictive scheme [DAS and Burgett 1993]. However, in both schemes, parameters were obtained on a block basis. The assumption here is that the block pixels possess stationary statistics. When this assumption fails, the situation is similar to simple DPCM; large prediction errors are obtained. The block size could be reduced at the expense of more side information.

The idea of switching the predictor in the hybrid SADPCM coder is by no means new; several schemes based on this idea have been reported in the literature [Prabhu 1985, Zschunke 1977]. The novelty of the scheme presented in this paper is that local shape is transmitted without much side information via VQ. VQ simplifies the process of selecting the appropriate predictor based on the decision rule and storing or transmitting the information through the index of the shape vector. Unlike DPCM, sudden changes in the image can be found precisely in the hybrid SADPCM scheme and the high activity components can be detected and decorrelated (see Table 3). The proposed hybrid scheme retains the good characteristics of pixel-based ADPCM; the drawback of huge side information is overcome by using VQ. When compared to block-based ADPCM, complex matrix computation is obviated, while prediction performance is improved by switching the predictors more finely on a pixel-by-pixel basis.

7. Simulation and Results

All the images tested here are 8 bits per pixel grey scale images, and their sizes are 256*256 pixels. Included in simulations are coders based on the lossless JPEG coder; the seven predictors,

Pixel	(a)	(b)	(c)	(d)	(e)	(f)	(g)	(h)	(i)
Error by DPCM	-104	125	-149	106	113	71	-85	-192	108
Predictor in SADPCM	VQ	First order	First order	First order	First order	Second order	VQ	First order	Second order
Error by SADPCM	-21	-9	-19	2	-4	13	9	-8	-1

Table 3. A comparison of prediction errors using DPCM and SADPCM.

Image / Method	Abdo	Feet	Head	Pelvis	Thighs	Jet	Lena	Baboon	Lax
J1	5.80	2.92	3.55	5.02	4.88	3.61	5.22	5.99	6.19
J2	5.43	2.39	3.35	4.52	4.07	3.74	4.61	5.74	6.40
J3	6.15	3.09	3.84	5.32	5.10	4.02	5.46	6.21	6.55
J4	5.04	2.27	3.09	4.23	3.89	4.01	4.74	6.03	6.44
J5	5.16	2.43	3.00	4.32	4.12	3.54	4.70	5.81	6.13
J6	4.93	2.26	3.43	4.00	3.68	3.58	4.55	5.93	6.19
J7	5.25	2.43	3.01	4.36	4.13	3.31	4.62	5.81	5.98
DPCM	5.00	2.25	3.07	4.20	4.10	4.00	4.71	6.39	5.99
ADPCM	4.81	2.35	2.98	3.98	3.92	3.55	4.61	5.82	5.63
MAR	4.82	2.48	3.10	4.20	3.85	3.79	4.20	6.22	5.91
HINT	5.09	2.37	3.04	4.22	3.86	3.44	4.46	5.94	5.65
SADPCM	4.73	2.24	2.97	3.98	3.66	3.29	4.28	5.69	5.23

Table 4. Results of compression (bits/pixel) with nine test images.

J1 – J7, listed in Table II of Aravind et al. [Aravind et al. 1993] are used. The ADPCM coder used in the simulation is the block-based scheme introduced by Kuduvalli and Rangayyan [Kuduvalli and Rangayyan 1992]. The MAR was by Das and Burgett reported as efficient in lossless image coding [Das and Burgett 1993]. The other two coding schemes, DPCM and HINT (see Table 4), are widely used in lossless coders [Kuduvalli and Rangayyan 1992, ROOS et al. 1988]. The results obtained for pixel-based ADPCM are not listed here, because their entropies are much higher than all the others when the side information is included.

The results quoted in the tables are the first-order entropy values of the errors with the side information added. The bits used for side information in the proposed scheme are calculated as: $\frac{8 * 1024 + 1 * 4096}{256 * 256} = 0.19$ bits/pixel, where 8*1024 is the contribution from the total bits used for the indices of 8*8 blocks (a total of 1024 blocks in a 256*256 image), and 1*4096 is the contribution from the bits used for the indices of 4*4 blocks. The results for nine test images are given in Table 4.

8. Discussion of Results

From the results listed in Table 4 it is fair to conclude that the proposed hybrid SADPCM coding scheme outperforms the traditional DPCM coder and HINT for all the images tested. Compared to DPCM, hybrid SADPCM shows an improvement ranging from 0.01 to 0.76 bits/pixel; a mean improvement of 0.4 bits/pixel. The performance of the proposed scheme with "complex " images such as "Lena", "Baboon " and "Lax " indicates that the scheme is better able to decorrelate high-activity images. This claim is corroborated by the performance of the scheme with "simple" images such as "Feet"; not much gain has been provided by the new scheme compared to DPCM because most regions of the "simple " image are classified as low-activity type and, as such, would have been decorrelated by the DPCM in the new scheme.

Compared to HINT and the best JPEG coder for each image, the proposed scheme can achieve about 5% improvement. It is worth mentioning here that Shen and Rangayyan [SHEN and RANGAYYAN 1997] reported that segmentation-based coding could improve the compression bit rate by about 29% and 13%, compared to JPEG and HINT. Simple regional growing technique in the segmentation-based scheme may also suggest its superiority in computational aspect. Nevertheless, the new shape-adaptive scheme still has novel ideas of extracting and describing the shape information by VQ and executing the pixel-by-pixel adaptive DPCM without much side information.

It appears that the new scheme can achieve better compression ratio than the ADPCM proposed by Kuduvalli and Rangayyan [Kuduvalli and Rangayyan 1992] or the MAR proposed by

Das and Burgett [Das and Burgeet 1993], and it has far less computation burden compared to ADPCM and MAR, as it does not have the complex matrix or recursive calculations.

Apart from investigating ways of adapting to local statistics of the image and minimising the mean squared prediction error, research effort needs to be directed at predictors maximising the entropy of the predicted values. This technique might lead to lossless image coders with a much reduced bit rate.

References

A. HABIBI, Comparison of nth-order DPCM encoder with linear transformations and block quantization techniques.,IEEE Transactions on Communication, Vol. Com–19 (1971), No. 6, 948–956

A. HABIBI, Survey of adaptive image coding techniques, IEEE Transactions on Communications, Vol. com–25 (1977), No. 11, 1275–1284.

A. K. JAIN, Fundamentals of digital image processing, Prentice–Hall, Inc., 1989.

C. H. HSIEH, P. C. LU AND W. G. LIOU, Adaptive predictive image coding using local characteristics, IEEE Proceedings, Vol. 136 (1989), Pt. I, No. 6, 385–390.

G. R. KUDUVALLI, AND R. M. RANGAYYAN, Performance analysis of reversible image compression techniques for high-resolution digital teleradiology. IEEE Transactions on Medical Imaging, Vol. 11 (1992), No. 3, 430–445.

K. A. PRABHU, A predictor switching scheme for DPCM coding of video signals, IEEE Transactions on Communications, Vol. com–33 (1985), No. 4, 373–379.

L. SHEN, AND R. M. RANGAYYAN, Segmentation-based lossless image coding method for high-resolution medical image compression, Vol. 16 (1997), No. 3, 301–307.

M. DAS AND S. BURGETT, Lossless compression of medical images using two-dimensional multiplicative autoregressive models, IEEE Transactions on Medical Imaging, Vol. 12 (1993), No. 4, 721–726.

P. A. MARAGOS, AND R. W. SCHAFER, R. M. MERSEREAU, Two-dimensional linear prediction and its application to adaptive predictive coding of images. IEEE Transactions on Acoustics, Speech, and Signal Processing, Vol. ASSP–32 (1984), No. 6, 1213–1229.

P. C. COWMAN, K. L. OEHLER, E. A. RISKIN AND R. M. GREY, Using vector quantization for image processing. Proceedings of the IEEE, Vol. 81 (1984), No. 9, 1326–1341.

P. ROOS, M. A. VIERGEVER, M. C. A. VAN DIJKE AND J. H. PETERS, Reversible intraframe compression of medical images, IEEE Transactions on Medical Imaging, Vol. 7 (1988), No. 4, 328–336.

R. ARAVIND, G. L. CASH, D. L. DUTTWEILER, H. HANG, B. G. HASKELL AND A. PURI, Image and video coding standards. AT&T Technical Journal, Vol. 72 (1993), #1, 67–89.

R. M. GREY, Vector quantization, IEEE ASSP Mag., Vol. 1 (1984), No. 2, 4–29.

W. ZSCHUNKE, DPCM picture coding with adaptive prediction, IEEE Transactions on Communications, Vol. com–25 (1977), No. 11, 1295–1302.

X. WU, Lossless compression of continuous-tone images via context selection, quantization, and modeling, IEEE Transactions on Image Processing, Vol. 6 (1997), No. 5, 656–664.

Received: May, 1997
Accepted: December, 1997

Contact address:
Jian Wang
Department of Electrical & Computer Engineering
University of Wollongong
Northfield Ave. NSW 2522
Australia
fax: +61-2-42213236
phone: +61-2-42214689
email: jiwa@st.elec.uow.edu.au

JIAN WANG received the BE degree in bio-medical engineering in 1993 at the Capital Institute of Medicine, Beijing, China. He is now pursuing his PhD study in the Department of Electrical & Computer Engineering, University of Wollongong, Australia. His research interests are in image compression, computer vision, and medical image processing.

PHILIP OGUNBONA received the BSc (Hons) degree in electronic and electrical engineering from University of Ife, Nigeria, in 1981 and the DIC, PhD in electrical engineering from Imperial College of Science, Technology and Medicine, University of London, United Kingdom, in 1987. He is currently a Senior Lecturer in the Department of Electrical & Computer Engineering, University of Wollongong, Australia. His current research interests include wavelets, image and video compression, and multimedia database. He is a member of IEEE.

GOLSHAH NAGHDY is a Senior Lecturer in the Department of Electrical & Computer Engineering, University of Wollongong, Australia. She received a BSc degree in electrical and electronic engineering from Aryamehr University of Technology in Tehran in 1977. She received a Mphil in control engineering from Bradford University and a PhD in electronic engineering from Portsmouth University, England, in 1982 and 1986, respectively. She was a senior lecturer at Portsmouth University before emigrating to Australia in 1989. Her research interests are in biological and machine vision and medical image processing.